Low-temperature magnetic relaxation in $HgBa_2Ca_2Cu_3O_{8+\delta}$ single crystals with columnar defects

E. R. Nowak,* J. M. Fabijanic, S. Anders, and H. M. Jaeger
James Franck Institute, The University of Chicago, Chicago, Illinois 60637
(Received 17 November 1997)

Micrometer-sized Hall probes are used to measure the low-temperature magnetic properties of $HgBa_2Ca_2Cu_3O_{8+\delta}$ single crystals with and without columnar defects. Introduction of columnar defects by heavy-ion irradiation suppresses the quasiexponential temperature dependence of the critical current, but only when the density of flux lines is less than the density of defects. The current-dependent creep activation energy $U(J)$ is found to be best described by the power law: $U(J)=U_0[(J_c/J)^{\mu}-1]$. At high current densities J, and low fields, there is a crossover to a quantum vortex creep process with a temperature-independent magnetic relaxation rate. On the low-J side of this crossover in the unirradiated sample, $\mu \geqslant 1$, indicating that the thermally activated vortex creep process is consistent with collective creep. When the flux-line density exceeds the columnar defect density in the irradiated sample, the vortex creep process is characterized by $\mu \sim 1$. For flux-line densities less than the defect density, an anomalously large exponent is found ($\mu \geqslant 2$), which is inconsistent with vortex transport occurring either by the nucleation and expansion of half-loop excitations or by variable-range hopping of vortex lines as described by the Bose-glass theory. [S0163-1829(98)08333-7]

The discovery of the mercury-based copper oxide superconductors[1] having transition temperatures $T_c \sim 130$ K has generated a great deal of interest, especially for technological applications. However, the viability of these compounds for applications will ultimately depend on their current carrying capabilities, and understanding and controlling magnetic flux creep that gives rise to decaying currents[2] and thermally activated resistance.[3] The giant flux creep present in the high-temperature superconductors[2] is a consequence of large thermal fluctuations, short coherence lengths, and strong anisotropy. The combination of these factors leads to intrinsically weak pinning of flux lines and thus low critical currents. To overcome this limitation, the conventional approach has been to deliberately engineer disorder into the materials. The presence of disorder, whether in the form of point or extended defects occurring naturally or introduced through either doping[4,5] or various forms of irradiation,[6,7] increases the barrier for flux line (vortex) motion and has been demonstrated to enhance important technological properties such as the critical current density J_c.

Due to the current unavailability of large $HgBa_2Ca_{n-1}Cu_nO_{2(n+1)+\delta}$ single crystals, nearly all studies of their magnetic properties have involved randomly oriented, polycrystalline[8–10] or grain-aligned samples.[11,12] Here, we denote the single CuO_2 layer compound with $n=1$, Hg-1201, the double layer $n=2$, as Hg-1212 and triple layer $n=3$, as Hg-1223. These studies have shown that the irreversibility lines of these compounds lie between that of the Bi- and Tl-based compounds and the more isotropic $YBa_2Cu_3O_{7-\delta}$. In addition, at intermediate and high temperatures the magnetic hysteresis and relaxation processes appear to be well described by the thermally activated penetration of two-dimensional pancake vortices over a Bean-Livingston surface barrier.[13] Neutron irradiation studies[14–17] have shown that Hg-1201 is not intrinsically limited to low current densities. Rather, the irradiation was found to suppress surface pinning, moderately enhance the critical current, and shift the irreversibility line to higher temperatures. High current densities have also been attained in *c*-axis oriented epitaxial films of Hg-1212.[18] These studies indicate that the Hg-based compounds can support large in-plane current densities at temperatures higher than has been achieved for other superconductors.

To date, studies analogous to neutron irradiation, but using high energy, heavy-ions have been unfeasible because heavy ions have a maximum range in solids of only 20–30 μm, making it virtually impossible to produce defects throughout macroscopic grain-aligned samples. (Recently, it was demonstrated that randomly oriented columnar defects can be created in Bi-based compounds by proton irradiation, which has a much longer penetration.[6,19]) Such heavy-ion irradiation creates defects in the form of cylindrical amorphous tracks (''columnar defects''). This is to be contrasted with neutron irradiation that produces defect cascades consisting of small volumes in which structural disordering and partial melting occur. Columnar defects provide the maximum pinning of flux lines because they match the linear geometry of flux lines, and their diameter ($\sim$10 nm) is comparable to the dimension of a vortex core. It is important then to determine how columnar defects affect vortex motion and whether such defects offer a substantial enhancement of the magnetic properties in comparison to defect cascades in these materials.

In this paper, we address these issues in single microcrystals of the $HgBa_2Ca_2Cu_3O_{8+\delta}$ compound (Hg-1223). Such crystals are sufficiently thin to ensure that irradiation creates columnar defects that extend entirely through the material. Using miniature Hall probes, we report measurements of the *local* magnetic induction B and its time decay for B along the length of the defects and parallel to the c axis. From the relaxation data we investigate the creep rate as a function of temperature and extract the current density and magnetic-field dependencies of the activation barrier.

Nearly 100% phase-pure Hg-1223 compounds were synthesized from appropriate mixtures of the corresponding metal oxide powders as described in Ref. 20. The as-synthesized samples were mechanically ground to free individual grains from the residual flux matrix. These grains were irregularly shaped platelets having lateral dimensions ranging from 10–25 μm and with thicknesses of 2 μm. Us-

ing a scanning electron beam, we examined the Kikuchi patterns[21] from such grains. In addition to identifying the orientation of the grains (the *c* axis was parallel to the thickness direction), the orientation of the Kikuchi pattern remained unchanged ($\pm 2°$) as the beam was rastered along the entire surface of the grain. This latter observation confirms that the grains were single crystals.

For the measurements, we chose crystals that were at least 10 μm on a side, and had regular shapes, e.g., rectangular-like. Some of these crystals were then irradiated at the ATLAS source with 800 MeV Ag ions directed along the *c* axis ($\pm 5°$). It is well established[7,22] that ionization energy loss by fast heavy ions can produce permanent damage effects in cuprate superconductors. Calculations using the TRIM Monte Carlo energy deposition routine[23] indicate that, within the thicknesses of our Hg-1223 crystals ($\leqslant 2$ μm), the energy deposition rate of the Ag ions is relatively constant at approximately 21 keV/nm. This ionization energy loss for Ag ions has previously been shown[22] to be sufficiently large for producing columnar defects with diameters ranging between 5–11 nm and penetration depths of ~ 16 μm in $YBa_2Cu_3O_{7-\delta}$ and $Bi_2Sr_2Ca_2Cu_3O_x$ samples. Although microstructural data on damage tracks in Hg-1223 crystals is not presently available, based on the above results the damage microstructure expected from the irradiation consists of continuous columns of amorphous material extending through our crystals and distributed randomly in the plane perpendicular to the ion beam. The ion flux dosage was chosen so that the number of columnar defects would equal the number of flux lines in a magnetic field of $B_\phi = 10\ \text{kG} \pm 2\ \text{kG}$.[24]

The present unavailability of larger crystals of the Hg-based compounds has limited experimental studies to grain-aligned samples. To overcome this restriction, we have used micron-sized Bi Hall probes to measure the local magnetization and magnetic relaxation in *single* crystals. The field sensitivity of these sensors (~ 1 G) allowed us to acquire reliable data below 20 K and for most applied magnetic fields parallel to the *c* axis. The crystals were centered directly on top of the Bi Hall probes and affixed by using a very thin layer (<1 μm) of grease. The field just at the surface of the crystal induces a Hall voltage that was calibrated to give the averaged local field *B* across the $3\ \mu\text{m} \times 3\ \mu\text{m}$ active areas of these probes. We define the magnetization as $M \equiv B - H$ and report the magnetic properties as a function of the local field *B* rather than the applied field *H*. (For irradiated samples, it was found that *B* is the relevant quantity on which many of the magnetic properties depend.[25,26]) All measurements were carried out under field-cooled conditions. In order to ensure that a well-defined flux density gradient was established (fully penetrated) throughout the crystal, the field was ramped over tens of kiloGauss (>20 kG) prior to starting all the measurements. Magnetic hysteresis, $M(B)$ loops, were recorded at a constant field sweep rate of 50 G/s at fixed temperatures. Likewise, isothermal magnetic relaxation measurements were performed by ramping the field over several Tesla at a rate of 50 G/s to various initial values of *B*.

The magnetic hysteresis loops were predominately symmetric about $M = 0$ for both types of samples at $T < 20$ K. This would suggest that, in comparison to bulk pinning, surface barriers contribute negligibly to the irreversible magnetization at these low temperatures. Other papers[12,27,28] on grain-aligned samples have found that surface barriers can significantly affect the field dependence of the magnetization to temperatures as low as 10 K. The enhanced bulk pinning is perhaps indicative that our pristine crystals were somewhat oxygen overdoped. The extremely small size of these crystals prevented direct measurements of T_c by conventional techniques as a means of checking stoichiometry.

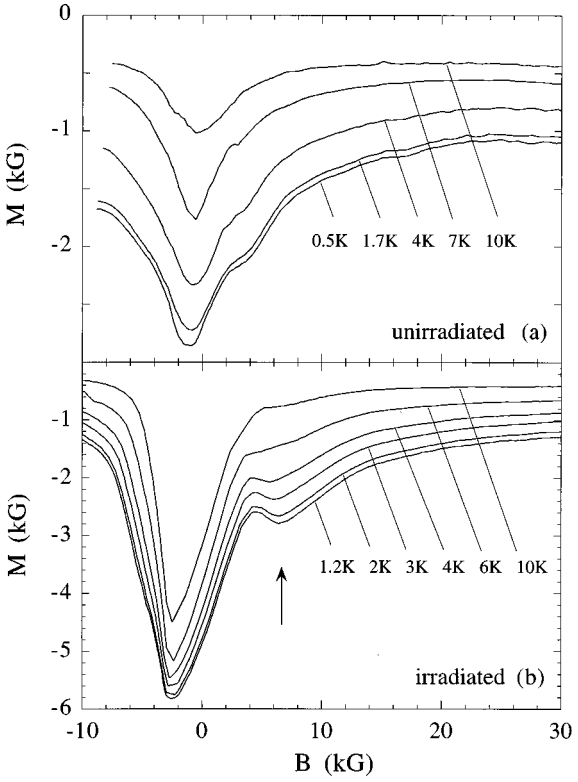

FIG. 1. Magnetization as a function of the internal field *B* for flux entry is shown at various temperatures for the (a) unirradiated and (b) irradiated single crystals. Columnar defects give rise to increased magnetization at low fields and a prominent peak near $B_\phi = 10\ \text{kG} \pm 2\ \text{kG}$ as indicated by the arrow in (b).

Irradiation is known to lead to an increase in the irreversible magnetization that can be related to the critical current density J_c, according to the Bean model.[29] In Fig. 1 we show one quadrant of the magnetization loop (for flux entry) at various temperatures for both the unirradiated and irradiated samples. Since the Hall probe measures the local field, we can, in principle, determine J_c directly through Maxwell's equation $J_c = (c/4\pi)dB/dx$.[30] However, even with our miniature Hall probes, the crystals were too small to allow for a direct measurement of the field gradient. Thus, we estimate J_c by $J_c \approx (c/4\pi)\Delta M/2L$, where $\Delta M = M_{\text{exit}} - M_{\text{entry}}$ is the width of the hysteresis loop at a local field *B* and *L* is the lateral distance of the Hall probe from the nearest edge of the crystal. $L \approx 10$ μm for both samples. Implicit in this expression for J_c is the assumption that the current is uniform across the sample. This, however, is not the case for samples with columnar defects for which there can exist two critical currents J_{c1} and J_{c2} in regions of the crystal where $B < B_\phi$ and $B > B_\phi$, respectively, with $J_{c1} > J_{c2}$.[31] This effect is minimized in our microcrystals for which the variation of *B* across the crystal is small. In addition, with the mag-

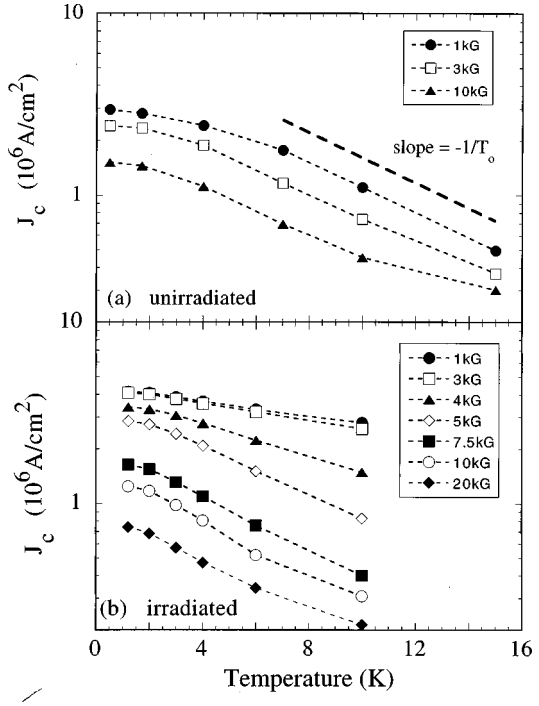

FIG. 2. The temperature dependence of the critical current at various internal fields B. For $T>3$ K, $J_c(T)$ can be approximated as $\propto \exp(-T/T_0)$ as indicated by the thick dashed line in (a). For the irradiated sample (b), T_0 is a strong function of field.

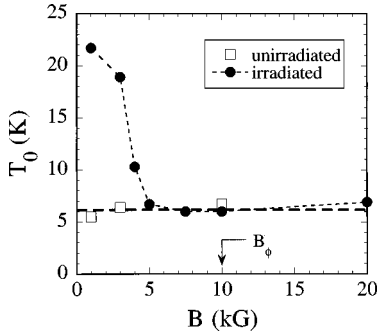

FIG. 3. The field dependence of the empirical parameter T_0 from Fig. 2. T_0 is a measure of the pinning strength. Columnar defects enhance T_0 for $B<B_\phi$, but are less effective at higher fields where the vortex density is comparable to or greater than the defect density. When $B>B_\phi$, the value of T_0 is not affected by irradiation.

netic field applied perpendicular to the plane of the crystal, demagnetization effects cause a bending of the field lines, resulting in a critical current that is not simply proportional to the gradient of the field. Nevertheless, near the center of the sample, where our Hall probe is positioned, the field lines are nearly straight. Hence, a local measurement of the internal magnetic field can provide a good estimate of J_c.

A characteristic feature of high-temperature superconductors is the large flux creep rate. Consequently, any measurement of J_c is a lower bound estimate of the true critical current, determined by the time scale of the measurement. We find a significant enhancement (factor of 2) of J_c after irradiation only for $B<B_\phi$: $J_c(T=2\text{ K},\ B=1\text{ kG})\approx 4\times 10^6$ A/cm^2 for the irradiated crystal. This enhancement factor may be a lower bound since our unirradiated crystals were found to sustain relatively large current densities. These large critical currents are due to an unknown defect structure, presumably preexisting point defects. In addition, the presence of columnar defects also introduces a nonmonotonic dependence to $M(B)$. This can seen in Fig. 1(b), where the magnetization has a local maximum at a field $B\approx 7$ kG, approximately equal to the matching field, $B_\phi=10$ kG ± 2 kG.[24] Such behavior has been discussed elsewhere[25,26] in the context of the Mott-insulator line phase that was proposed by Nelson and Vinokur[32,33] to exist within the Bose-glass phase for vortices.

The temperature dependence of J_c is shown in Fig. 2. The field resolution of the Hall probe and the small size of the crystals restricted the data to a narrow range of temperatures. Even so, several features are apparent. At low temperatures and fields, $J_c(T)$ is found to level off, becoming nearly temperature independent. [For the irradiated crystal, J_c is expected to show a nonmonotonic dependence on field, similar to the magnetization. This dependence is absent in Fig. 2(b) because the fine features in the magnetization loops for flux entry and flux exit are not symmetric, and J_c is calculated from the total width of the hysteresis loop.] At high temperatures, $J_c(T)$ can be described by an exponential dependence $J_c\propto\exp(-T/T_0)$.[34,35] The empirical parameter T_0 is a measure of the pinning strength. We find that $T_0\approx 20$ K in the irradiated crystal for $B<B_\phi$ and drops rapidly with increasing field. For $B>B_\phi$, T_0 approaches the value found in the unirradiated sample, where $T_0\approx 6$ K, as shown in Fig. 3. Previous studies on Hg-1223 powder samples indicate values ranging from $11\text{ K}<T_0<17$ K for grain-aligned samples[12,15,27] to 7 K for randomly oriented crystallites.[10] In one study neutron irradiation was found to increase T_0 from 11 to 17 K.[15] By comparison, columnar defects suppress the temperature dependence of J_c by a factor of >3, at least for low fields, where the density of flux lines is less than the density of defects.

The time evolution of magnetization $M(t,B,T)$ was recorded over times $10<t<10^5$ s along the diamagnetic branch of the hysteresis loop. For the irradiated crystal this is not the branch shown in Fig. 1(b) but that corresponding to negative applied fields. This branch did not show the strong nonmonotonic dependence of $M(B)$ evident in Fig. 1(b).[36] The inset to Fig. 4 shows that the magnetization decay can be considerable over the experimental time window. Except for the lowest temperatures and fields, the decay of the magnetization in both unirradiated and irradiated crystals was not found to be logarithmic in time. Nor was it consistent with an exponential decay to an equilibrium magnetization, as might be expected at long times in the standard model of flux creep by Anderson-Kim.[37] A nonlogarithmic decay is generally attributed to the current dependence of the activation barrier for flux creep $U(J)$.[2]

To examine the temperature dependence of the flux creep rate, we plot in Fig. 4 the normalized creep rate $S=-d\ \ln(M)/d\ \ln(t)$ averaged over times $10<t<5000$ s. At the lowest temperatures and fields, S takes on a finite and temperature-independent value, as denoted by the dashed lines. Such behavior has previously been taken as evidence for vortex motion that is not thermally activated but occurs by quantum tunneling.[17,38–40] The crossover to quantum tunneling of vortices occurs below $T\sim 2$ K for the unirriadated

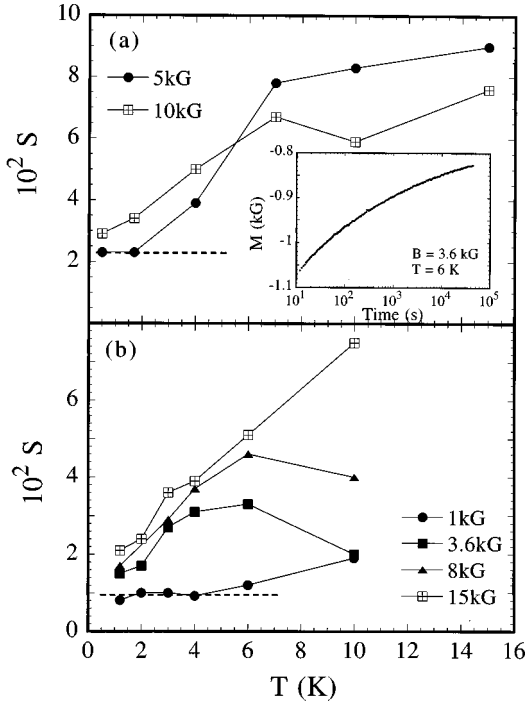

FIG. 4. The temperature dependence of the normalized relaxation rate $S=-d\ \ln(M)/d\ \ln(t)$ is plotted at various values of the initial internal field B for the (a) unirradiated and (b) irradiated samples. The inset shows the large and typically nonlogarithmic magnetic relaxation for the irradiated sample. At low T and B, S approaches a finite and temperature-independent value, indicated by the thick dashed lines.

sample at $B=5$ kG and as high as ~ 4 K in the presence of columnar defects at $B=1$ kG. At higher fields the creep rate is larger and $S(T)$ is nearly linear in T. These curves tend to merge at low T, approaching a finite value as $T\rightarrow 0$. Indeed, extrapolation of S to $T=0$ at higher fields yields values for $S(0)$ that are nearly equivalent to the quantum creep rate found at the lowest field in each sample. Field independence of the quantum creep rate suggests that the single vortex regime for pinning applies. In general, $S(T)$ is an increasing function of temperature, though not strictly monotonic. Although the low-temperature features of the vortex creep rate are similar to those found in randomly oriented[40] and neutron irradiated, grain-aligned samples,[17] the form of $S(T)$ for $T>15$ K differs strongly amongst samples and requires further investigation.

Figure 4 indicates that the magnitude and temperature dependence of the flux creep rate is modestly reduced by the introduction of parallel columnar defects. We note, however, that the relaxation process is determined by the activation barrier U, which is a function of the current density J. As shown in Fig. 1, irradiation can increase J, which affects U and the creep rate. Thus, a proper evaluation requires comparison of U at the same current densities (see below).

We now address the question of how the presence of columnar defects affects vortex creep in these compounds. One approach is to use the interpolation formula $M(t)=M_0/[1+(\mu kT/U_0)\ln(t/t_0)]^{1/\mu}$, which is applicable for both the vortex-glass[41] and collective pinning models.[42–44] Here, t_0 is a macroscopic, effective time scale, M_0 is the initial magnetization, and the exponent μ characterizes the creep process. By way of determining the normalized relaxation rate, we observed a decrease of S proportional to the logarithm of time. This indicates that an effective barrier for flux creep increases with decreasing persistent current, as predicted by the interpolation formula. By plotting $M^{-\mu}$ as a function of $\ln(t)$ and doing least-squares fits to the expression $M(t)^{-\mu}=M_0^{-\mu}+c(T)\ln(t)$, we obtained values for the exponent $\mu(T,B)$ and the other fitting parameters M_0 and $c(T)$. Determined in this way, $\mu\leqslant 1$ at low temperatures and fields and predominately increased with increasing B and T. For the three-dimensional (3D) collective pinning case in the low-field, low-temperature region where the creep is dominated by the motion of individual flux lines, $\mu=\frac{1}{7}$. At higher temperatures and fields the exponent attains its maximum value of $\mu=\frac{3}{2}$ due to collective creep of bundles. One troubling aspect is that the fits often yielded $\mu>3$, a value greater than could be accounted for by the theory.[45] Nevertheless, using these values of μ we made fits to the decay curves. However, the limited time window of the measurements and the remaining three parameters allowed for considerable latitude in obtaining an optimal fit. Consequently, we were unable to unambiguously determine how these parameters changed with temperature or field.

The nature of the vortex creep process is perhaps best revealed by the current-dependent creep activation barrier $U(T,J)$.[11] $U(J)$ can be determined from the magnetic relaxation data by using either the method put forth by Maley *et al.*[46] or the generalized inversion scheme.[47] The latter scheme was developed to extract $U(T,J)$ without assumptions of the functional form of the temperature dependence. Here, we use the Maley analysis and assume that U is independent of temperature. This is a reasonable assumption for our experimental regime, which is far below the irreversibility temperature $T_{\rm irr}>90$ K, for which all thermal factors such as the condensation energy are nearly constant. Briefly, this procedure uses the flux conservation equation and the Arrhenius law for flux hopping to derive the master rate equation $U(J,T)=-kT[\ln(dM/dt)-C]$. Here $C=\ln(B\omega a/\pi L)$ is a temperature-independent constant uniquely fixed by requiring that, at low temperatures, U is a continuous function of J, $\omega=2\pi/\tau_0$ is a microscopic attempt frequency, a is the hop distance, and L is the sample dimension, as before. The construction of U with several segments is valid only at low temperatures where the temperature dependence of the barrier is negligible and the vortex motion is classical.[34] Thus, we require ''piecewise'' continuity only for segments taken at $T>3$ K for which the vortex motion was dominated by thermal activation rather than quantum tunneling, see Fig. 4. The optimal value of C was 19 and 25 for the unirradiated and irradiated samples, respectively. We find that for both unirradiated and irradiated samples the functional form for $U(J)$ is best described by a power law[32,41,45] as given by

$$U(J,T)=U_0(T)[(J_c/J)^{\mu}-1], \tag{1}$$

rather than a logarithmic dependence $U(J)\propto\ln(J_c/J)$ as seen in Refs. 48 and 49. Both power-law and logarithmic dependences have been observed in neutron irradiated[17] and unirradiated[50,51] grain-aligned samples, respectively. At the lowest temperatures (highest J) there is a strong reduction of

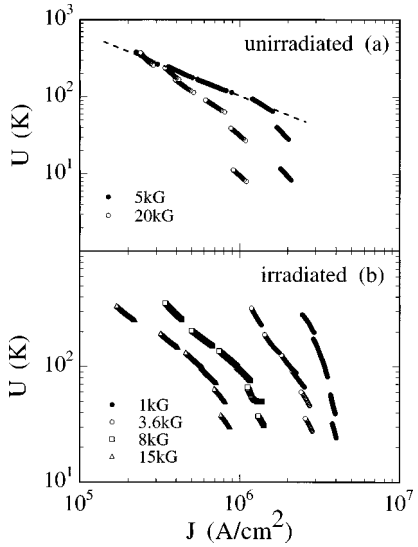

FIG. 5. The current dependence of the activation barrier $U(J)$ extracted from the magnetic relaxation data at various internal fields B and temperatures. In order of increasing J, the segments correspond to relaxation data taken at $T=15$, 10, 7, 4, 1.7, and 0.5 K in (a) and 10, 6, 4, 3, 2, and 1.2 K in (b). The two segments corresponding to the lowest values of U at each B were not included in the inversion scheme. At those temperatures, $T<3$ K, quantum tunneling of flux lines vortex motion appears to dominate the flux creep. For $T>3$ K, $U(J)$ is best fit by a power law, see, e.g., the dashed line in (a).

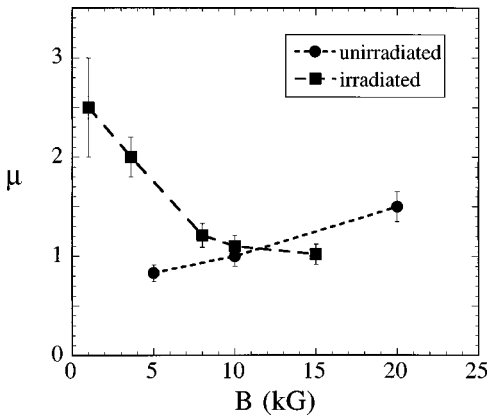

FIG. 6. The μ values extracted from a fit to Eq. (1) for the high-temperature (low J) segments in Fig. 5. $\mu(B)$ increases monotonically for the unirradiated sample. In the irradiated sample, $\mu(H)$ drops rapidly as $B\rightarrow B_\phi$, and approaches values comparable to those found in the unirradiated sample.

U that reflects the process of quantum creep, see Figs. 5(a) and 5(b). Quantum creep gives a finite creep rate even as $T\rightarrow 0$, resulting in $U\approx T/S\rightarrow 0$. Hence, fits to Eq. (1) show strong deviations at the highest currents corresponding to the quantum creep regime.

The glassy exponent μ in Eq. (1) is regime specific and can be used to characterized the creep process. In the activated regime ($T>3$ K) $J\ll J_c$. Hence, $\ln U(J)\cong\ln U_0+\mu(\ln J_c-\ln J)$ and thus $\Delta \ln U/\Delta \ln J=\mu$. We estimate μ from Fig. 5 by taking the best fit through the data, excluding the segments from the quantum creep regime ($T<3$ K), for an example, see the dashed line in Fig. 5(a). Figure 6 shows how μ depends on B for both the irradiated and unirradiated samples. For the unirradiated sample $\mu(B=5\text{ kG})\sim 0.85$ and increases to $\mu(B=20\text{ kG})\sim 1.5$. Within the 3D collective pinning model this increasing trend with field suggests a crossover from the motion of individual flux lines to collective creep of small bundles. Our data are not sufficiently comprehensive to discriminate between three- and two-dimensional creep by ''pancake'' vortices, for which $\mu=\frac{9}{8}$.

By comparison, in the irradiated sample $\mu\sim 2.5$ at low fields and decreases sharply just below B_ϕ, approaching values ~ 1. In the Bose-glass scenario,[32] the vortex creep process is viewed as a sequence of nucleation of half-loop excitations and the subsequent expansion of half loops with decaying currents. This process is characterized by an exponent $\mu\sim 1$, consistent with the experimental results for $B\geqslant B_\phi$. However, the large value of μ for $B<B_\phi$ is difficult to reconcile with theory that predicts vortex transport to occur either by half-loop excitations or by variable-range hopping (VRH) of vortex lines,[32] which is characterized by $\mu\sim\frac{1}{3}$. Dispersion of flux-line binding energies to columnar defects can lead to VRH for which vortex motion occurs by hopping to a lower-energy defect that is far away rather than to a nearest neighbor, but higher-energy defect. Variable-range vortex hopping was recently found in $YBa_2Cu_3O_{7-\delta}$ crystals at low fields, $B<B_\phi$.[11] We find no evidence of a distinct power-law regime with $\mu=\frac{1}{3}$ over our experimental range for either $B=1$ or 3.6 kG. One possible explanation is that the VRH regime in Hg-1223 crystals occurs at current densities below our experimental resolution. On the other hand, if the objects that are hopping are ''pancake'' vortices, then VRH may not be as relevant since the dispersion in pancake binding energies should be smaller and the energy cost for a pancake vortex jumping into a higher-energy defect is much lower than that for a flux line.

Finally, we return to examining the effect of heavy-ion irradiation on the magnetic relaxation rate. Figure 4 shows that at low T and B, the quantum creep is nearly a factor of 2 lower in the presence of columnar defects where $S\sim 1\%$. This value is comparable to that found for quantum creep in other studies of Hg-1223.[17,40] The creep rate at higher T and B also remains lower in the irradiated sample, but is not strikingly reduced. Figure 5 indicates that, indeed, the effective barrier at a particular current density $U(J)$ is enhanced by columnar defects. For example, $U(J,B)=100$ K occurs at approximately 30–40 % higher current densities for the irradiated sample at an equivalent internal field. This apparently indicates that the irradiation affects U directly and not only through J.

In conclusion, we have found that the thermally activated flux creep in single crystals of the Hg-1223 compound with and without columnar defects can be described by an activation barrier that increases with time or with decreasing persistent current as a power-law given by Eq. (1). Moreover, the experimental results for the unirradiated crystal are consistent with collective flux creep theory. In general, the creep rate was found to be an increasing function of temperature. As $T\rightarrow 0$, we observed a finite creep rate that is temperature and nearly field independent and is attributed to the quantum tunneling of flux lines. Most striking was the strong suppression (factor of 3) of the temperature dependence of the critical current for columnar defects as compared to

neutron irradiation, but only for flux-line densities less than the density of defects.

We thank D. G. Hinks at Argonne National Laboratory for providing the Hg-1223 powder. We also thank W. K. Kwok, J. A. Fendrich, and B. Glagola (ANL) for assistance with performing the heavy-ion irradiation at the ATLAS source. This work was supported by the National Science Foundation (Grant No. DMR91-20000) through the Science and Technology Center for Superconductivity.

*Present address: University of Illinois, Loomis Laboratory of Physics, Urbana, Illinois 61801.

[1] S. N. Putilin, E. V. Antipov, O. Chmaissem, and M. Marezio, Nature (London) **362**, 227 (1993).
[2] Y. Yeshurun, A. P. Malozemoff, and A. Shaulov, Rev. Mod. Phys. **68**, 911 (1996).
[3] M. Tinkham, Phys. Rev. Lett. **61**, 1658 (1988).
[4] L. M. Paulius, C. C. Almasan, and M. B. Maple, Phys. Rev. B **47**, 11 627 (1993).
[5] P. L. Paulose, S. Patil, H. Frank, and G. Guntherodt, Physica C **208**, 11 (1993).
[6] H. Safar, J. H. Cho, S. Fleshler, M. P. Maley, J. O. Willis, J. Y. Coulter, J. L. Ullmann, G. N. Riley, M. W. Rupich, J. R. Thompson, and L. Krusin-Elblaum, Appl. Phys. Lett. **67**, 130 (1995).
[7] R. Wheeler, M. A. Kirk, A. D. Marwick, L. Civale, and F. H. Holtzberg, Appl. Phys. Lett. **63**, 1573 (1993).
[8] A. Schilling, O. Jeandupeux, J. D. Guo, and H. R. Ott, Physica C **216**, 6 (1993).
[9] U. Welp, G. W. Crabtree, J. L. Wagner, D. G. Hinks, P. G. Radaelli, and B. Dabrowski, Appl. Phys. Lett. **63**, 693 (1993).
[10] U. Welp, G. W. Crabtree, J. L. Wagner, D. G. Hinks, P. G. Radaelli, and B. Dabrowski, Physica C **218**, 373 (1993).
[11] J. R. Thompson, L. Krusin-Elbaum, L. Civale, G. Blatter, and C. Feild, Phys. Rev. Lett. **78**, 3181 (1997).
[12] J. A. Lewis, V. M. Vinokur, J. Wagner, and D. Hinks, Phys. Rev. B **52**, R3852 (1995).
[13] L. Burlachov, V. B. Geshkenbein, A. E. Koshelev, A. I. Larkin, and V. M. Vinokur, Phys. Rev. B **50**, R16 770 (1994).
[14] J. Schwartz, S. Nakamae, G. W. Raban Jr., J. K. Heuer, S. Wu, J. L. Wagner, and D. G. Hinks, Phys. Rev. B **48**, 9932 (1993).
[15] Y. R. Sun, K. A. Amm, and J. Schwartz, IEEE Trans. Appl. Supercond. **5**, 1870 (1995).
[16] K. M. Amm and J. Schwartz, J. Appl. Phys. **78**, 2575 (1995).
[17] S. Gjolmesli, K. Fossheim, Y. R. Sun, and J. Schwartz, Phys. Rev. B **52**, 10 447 (1995).
[18] L. Krusin-Elbaum, C. C. Tsuei, and A. Gupta, Nature (London) **373**, 679 (1995).
[19] L. Krusin-Elbaum, J. R. Thompson, R. Wheeler, A. D. Marwick, C. Li, S. Patel, D. T. Shaw, P. Lisowski, and J. Ullmann, Appl. Phys. Lett. **64**, 3331 (1994).
[20] J. L. Wagner, P. G. Radaelli, D. G. Hinks, J. D. Jorgensen, F. Mitchell, B. Dabrowski, G. S. Knapp, and M. A. Beno, Physica C **210**, 447 (1993).
[21] D. J. Dingley and V. Randle, J. Mater. Sci. **27**, 4545 (1992).
[22] Y. Zhu, Z. X. Cai, R. C. Budhani, M. Suenaga, and D. O. Welch, Phys. Rev. B **48**, 6436 (1993).
[23] J. F. Ziegler, J. P. Biersack, and U. Littlemark, *The Stopping and Range of Ions in Solids* (Pergamon, New York, 1985).
[24] In contrast to Au, where each ion produces a single columnar defect, the probability of forming columnar defects with Ag can be as low as 50%, see Ref. 22.
[25] E. R. Nowak, S. Anders, H. M. Jaeger, J. A. Fendrich, W. K. Kwok, R. Mogilevsky, and D. G. Hinks, Phys. Rev. B **54**, R12 725 (1996).
[26] K. M. Beauchamp, T. F. Rosenbaum, U. Welp, G. W. Crabtree, and V. M. Vinokur, Phys. Rev. Lett. **75**, 3942 (1995).
[27] Y. C. Kim, J. R. Thompson, D. K. Christen, Y. R. Sun, M. Paranthaman, and E. D. Specht, Phys. Rev. B **52**, 4438 (1995).
[28] G. C. Kim and Y. C. Kim, Physica C **259**, 218 (1996).
[29] C. P. Bean, Phys. Rev. Lett. **8**, 250 (1962).
[30] Y. Abulafia, A. Shaulov, Y. Wolfus, R. Prozorov, L. Burlachkov, Y. Yeshurun, D. Majer, E. Zeldov, and V. M. Vinokur, Phys. Rev. Lett. **75**, 2404 (1995).
[31] K. M. Beauchamp, L. Radzihovsky, E. Shung, T. F. Rosenbaum, U. Welp, and G. W. Crabtree, Phys. Rev. B **52**, 13 025 (1995).
[32] D. R. Nelson and V. M. Vinokur, Phys. Rev. Lett. **68**, 2398 (1992).
[33] D. R. Nelson and V. M. Vinokur, Phys. Rev. B **48**, 13 060 (1993).
[34] M. E. McHenry, S. Simizu, H. Lessure, M. P. Maley, J. Y. Coulter, I. Tanaka, and H. Kojima, Phys. Rev. B **44**, 7614 (1991).
[35] D. K. Christen and J. R. Thompson, Nature (London) **364**, 98 (1993).
[36] Demagnetization effects from the sample may account for such asymmetries and can be minimized by positioning the Hall probe at the center of a regularly shaped crystal, see Ref. 26.
[37] P. W. Anderson and Y. B. Kim, Rev. Mod. Phys. **36**, 39 (1964).
[38] L. Fruchter, A. P. Malozemoff, I. A. Campbell, J. Sanchez, M. Konczykowski, R. Griessen, and F. Holtzberg, Phys. Rev. B **43**, 8709 (1991).
[39] D. Prost, L. Fruchter, I. A. Campbell, N. Motohira, and M. Konczykowski, Phys. Rev. B **47**, 3457 (1993).
[40] X. X. Zhang, A. Garcia, J. Tejada, Y. Xin, G. F. Sun, and K. W. Wong, Phys. Rev. B **52**, 1325 (1995).
[41] D. S. Fisher, M. P. A. Fisher, and D. A. Huse, Phys. Rev. B **43**, 130 (1991).
[42] T. Natterman, Phys. Rev. Lett. **64**, 2454 (1990).
[43] M. V. Feigel'man, V. B. Geshkenbein, and V. M. Vinokur, Phys. Rev. B **43**, 6263 (1991).
[44] G. Blatter, M. V. Feigel'man, V. B. Geshkenbein, A. I. Larkin, and V. M. Vinokur, Rev. Mod. Phys. **66**, 1125 (1994).
[45] M. V. Feigel'man, V. B. Geshkenbein, A. I. Larkin, and V. M. Vinokur, Phys. Rev. Lett. **63**, 2303 (1989).
[46] M. P. Maley, J. O. Willis, H. Lessure, and M. E. McHenry, Phys. Rev. B **42**, 2639 (1990).
[47] H. G. Schnack, R. Griessen, J. G. Lensink, and H.-H. Wen, Phys. Rev. B **48**, 13 178 (1993).
[48] E. Zeldov, N. M. Amer, G. Koren, A. Gupta, R. J. Gambino, and M. W. McElfresh, Phys. Rev. Lett. **62**, 3093 (1989).
[49] E. Zeldov, N. M. Amer, G. Koren, A. Gupta, M. W. McElfresh, and R. J. Gambino, Appl. Phys. Lett. **56**, 680 (1990).
[50] G. C. Kim and Y. C. Kim, Jpn. J. Appl. Phys., Part 1 **34**, 6026 (1995).
[51] Y. Rui, H. L. Ji, X. N. Xu, H. M. Shao, M. J. Qin, X. Jin, X. X. Yao, X. S. Rong, B. Ying, and Z. X. Zhao, Phys. Rev. B **51**, 9161 (1995).